ACES Asian Chemical Editorial Society

DOI: 10.1002/cnma.201600004

CHEMNANOMAT
Communication

Nanoelectronics

SPECIAL ISSUE

Preparation of Highly Monodisperse Electroactive Pollen Biocomposites

Jeongeun Seo[+],[a] Lili Wang[+],[a, d] WeiBeng Ng,[a] and Nam-Joon Cho*[a, b, c]

Abstract: Sunflower pollen (SFP) was used as a novel biotemplate to fabricate nanoporous and spiked particles coated with carboxyl-functionalized multiwalled carbon nanotubes (COOH-MWCNTs). The MWCNT coating on SFPs was characterized by scanning electron microscopy, dynamic imaging particle analysis and Raman spectroscopy. The electrical properties of MWCNT-coated SFPs offer great potential to develop highly functional materials for electronics and optical applications.

With continued innovations in materials science, robust biocompatible composites have received much attention due to their tailorable and multifunctional physical and chemical properties that enable promising applications in supercapacitors, polyactuators, catalysis, electronic sensors, biosensors and bioimaging.[1] In particular, electroconductive composites combining carbon materials and biopolymers with a hierarchical structure have been reported to have excellent electrical conductivity and mechanical properties compared with nonfunctionalized biopolymers.[2] For example, Yang and co-workers reported the synthesis of polyphenylene sulfide–nanotube composites by a simple mixing and compression method, yielding a material which exhibited enhanced conductive properties.[3] Presently, a number of methods, such as covalent functionalization and noncovalent modification, are available to realize carbon-based polymer composites with excellent mechanical and conductive performances.[1b,4] However, the synthesis of electroconductive biocompatible composite materials by a simple method remains a technological challenge.

Nature offers various excellent biotemplates with precise widths and lengths and uniform geometries, such as diatoms, yeasts, butterfly wings and pollen grains.[5] Above all, pollen grains are attracting significant attention owing to their nontoxicity, high surface area and large pore volumes. These unique microstructures have inspired researchers to develop a variety of applications such as supercapacitors,[6] lithium ion batteries[7] and gas sensors.[8] Moreover, the carbon-based polymer additives with the greatest potential are carbon nanotubes (CNTs).[9] Key attributes of CNTs include intrinsically large surface areas and intriguing electrical properties that are motivating the development of new industrial products.[10] CNTs have become one of the main additives in polymer-composite fabrication because they are easy to produce and inexpensive.[11]

Herein, we describe a unique method for preparing electroactive sunflower pollen (SFP) grains based on high-efficiency surface functionalization with carboxyl-functionalized multiwalled CNTs (COOH-MWCNTs). We introduce sodium dodecyl sulfate (SDS) into the precipitation process in order to endow hydrophilic chains on the surface of the pollen grains that serve as surfactants to enhance hydrophilic properties. SFP is used as a novel biotemplate material to fabricate nanoporous and spiked electroactive microspheres. The fabrication process and control of each step are shown in Figure 1 (a, b).

The fabrication process has a two-step procedure comprising: 1) SDS functionalization of the surface of the pollen by electrostatic interactions and 2) synthesis of MWCNT-coated SDS-functionalized pollen with a high density using COOH-MWCNTs under specific pH conditions. The key to this process is the use of SFPs rich with surface functional groups available for adsorption of target compounds.[1b,12] Many studies on the fabrication of biocomposites (e.g., SDS-coated alumina)[13] demonstrate that SFPs rich with surface functional groups can absorb significant amounts of target compounds. The present aqueous-based chemical synthesis method is fast, simple, economical and environmentally mild. In particular, the main advantage of the method is that it occurs under ambient pressure and temperature conditions. The obtained SFP porous microspheres with an urchin-like structure are loaded with

[a] *Dr. J. Seo,[+] Dr. L. Wang,[+] W. Ng, Prof. N.-J. Cho*
School of Materials Science and Engineering
Nanyang Technological University
50 Nanyang Avenue, Singapore 639798 (Singapore)
E-mail: njcho@ntu.edu.sg

[b] *Prof. N.-J. Cho*
Centre for Biomimetic Sensor Science
Nanyang Technological University
50 Nanyang Drive, Singapore 637553 (Singapore)

[c] *Prof. N.-J. Cho*
School of Chemical and Biomedical Engineering
Nanyang Technological University
62 Nanyang Drive, Singapore 637459 (Singapore)

[d] *Dr. L. Wang[+]*
State Key Laboratory on Integrated Optoelectronics
College of Electronic Science and Engineering
Jilin University
Changchun, 130012 (China)

[+] *These authors contributed equally to this work.*

Supporting information for this article can be found under http://dx.doi.org/10.1002/cnma.201600004.

This manuscript is part of a Special Issue on Nanobiointerfaces. Click here to see the Table of Contents of the special issue.

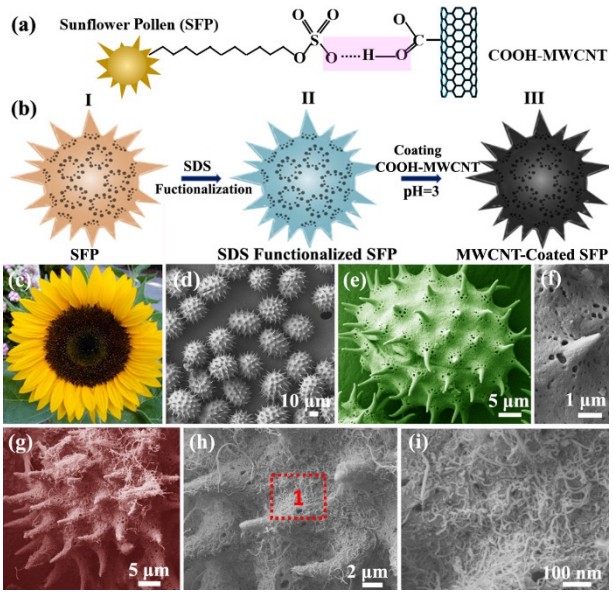

Figure 1. (a) Schematic illustration of the COOH-MWCNT coating fabrication strategy on SFP grains. (b) (I) Pollen with uniform spike ornamentation suspended in an SDS solution for adsorption by electrostatic interaction. (II and III) SDS-functionalized pollen grains coated with COOH-MWCNTs at pH 3 due to interaction between SDS-functionalized pollen and COOH-MWCNTs. (c) Optical photograph of sunflower. (d) FESEM image of an SFP grain with characteristic spike microstructure. (e, f) Magnified FESEM images showing the pollen surface with pores surrounding an individual spike. (g) FESEM image of a single MWCNT-coated SFP. (h) Magnified FESEM image of one area of the MWCNT-coated SFP with the area in the red square magnified in (i).

MWCNTs, with the density of the surface coating controlled by the solution pH at the deposition stage. The 3D hierarchical SFP-MWCNT microspheres show excellent electrical characteristics.

As illustrated in the scheme in Figure 1 (a, b), we designed a two-step procedure to fabricate the biocompatible material. Figure 1 (c–i) shows the experimental realization of Figure 1 (a, b) (see Supporting Information for experimental details). It is well-known that SFP is produced by the anthers of sunflowers (Figure 1 (c)). Each anther can carry up to 100 000 grains of pollen and is thus quite prolific. First, the morphology and structure of the SFP biomaterials are analyzed and characterized by field emission scanning electron microscopy (FESEM), as shown in Figure 1 (d–f). Interestingly, pure SFP grains are highly monodisperse large-size particles with a diameter of ca. 34.5 μm and a uniform hierarchical urchin-like structure with a spiky appearance. Further details of the surface structure can be directly examined in the magnified FESEM image (Figure 1 (f)). High uniformity of the hierarchical SFP structure is shown, and the spikes as well as porous structure are clearly revealed by the sharp contrast between the height of the outer and inner surfaces of the SFP. The surface is uniformly covered with spikes ca. 1.5–2 μm in height and numerous pores. MWCNTs are then deposited on the SFP microspheres to form well-coated shells (Figure 1 (g–i)).[14] A magnified image (Figure 1 (i)), taken from a specific area of Figure 1 (h), shows that the MWCNTs have an obvious nanotube structure and are randomly dispersed on the SFP surface. Although dispersed randomly, the nanotube structure is still able to maintain monodisperse character without apparent agglomeration, which is particularly favorable for various applications where a high surface area is desirable.

The pH value plays a key role in facilitating the interaction between the SDS-functionalized SFPs and COOH-MWCNTs. Therefore, the structure of the biocomposite materials under different pH conditions from 3 to 11 was analyzed in order to determine an optimal pH value, and the results are shown in Figure 2. Because SDS surfactants have a pK_a value around 2,

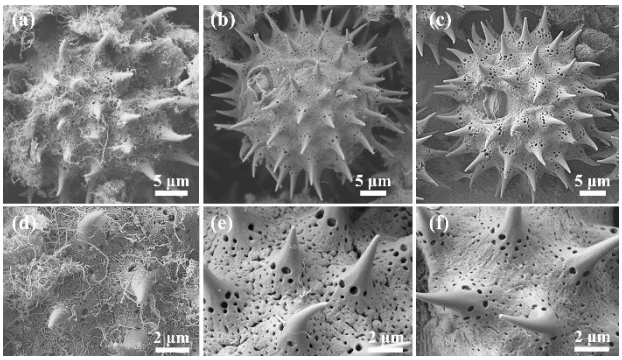

Figure 2. FESEM images of SFP grains after COOH-MWCNT coatings at different pH values: (a, d) pH 3.0; (b, e) pH 7.0; (c, f) pH 11.0.

they are negatively charged across all test conditions.[12] On the other hand, the COOH functional groups on the MWCNT surface have a pK_a value around 5.[15] Hence, at pH 3, the COOH functional groups on the MWCNTs are protonated and the MWCNTs have a neutral character. Under this acidic condition, nonelectrostatic forces (hydrogen bonding) likely drive the interaction between SDS-coated SFPs and COOH-MWCNTs (Figure 1 a). Figure 2 (a, d) shows FESEM images of MWCNT-coated SFPs at pH 3.0 in which it can be clearly seen that numerous MWCNTs have randomly deposited on the SFP microspheres. It can also be seen that the structure of the MWCNTs (Figure S1 in the Supporting Information) did not change after being coated on the SFPs. On the other hand, when the pH value is 7.0, a fraction of the COOH functional groups on the MWCNT are deprotonated and the MWCNTs are negatively charged. In this case, electrostatic repulsion between the negatively charged SDS and COOH-MWCNTs is the main force that impedes MWCNT adsorption onto the SFP surface. The FESEM images in Figure 2 (b, e) show a low density of coated MWCTs on the SFP. When the pH value is further increased to 11.0, electrostatic repulsion becomes greater due to a larger fraction of deprotonated COOH groups on the MWCNT surface. As such, the surface of the SFP becomes relatively clean, and the porous structures on the surface of SFP can be clearly observed (Figure 2 (c, f)). To further understand the significance of SDS in the coating process, we investigated the preparation of MWCNT-coated SFPs without surfactant or with cetyltrimethylammonium bromide (CTAB) under different pH conditions (for FESEM images of MWCNT-SFP using CTAB and without surfac-

tant at pH levels from 3.0 to 11.0, see Figure S2). Negligible MWCNT coating was observed under these other test conditions, supporting that SDS is a necessary part of the surface functionalization scheme and is involved in the interaction with the COOH-MWCNTs.

Changes in the surface and size properties of SFP grains before and after coating with MWCNTs were evaluated by dynamic image particle analysis (DIPA) (Figure 3). Representative images of pristine SFPs and MWCNT-coated SFPs are shown in

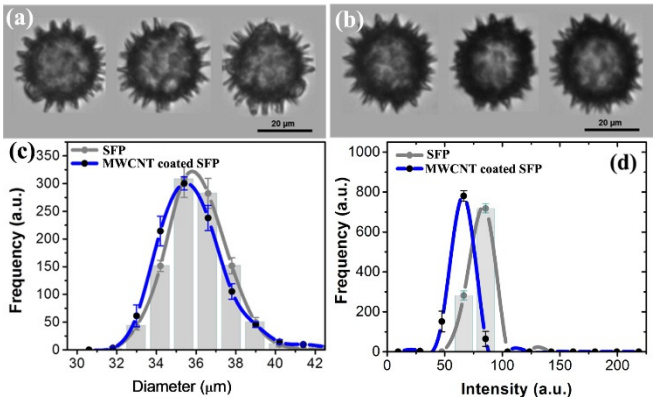

Figure 3. Dynamic imaging particle analysis (DIPA) images of sunflower pollen (SFP) grains. (a) SFP. (b) MWCNT-coated SFP. (c) Diameter and (d) transparency of SFP grains before and after COOH-MWCNT coating as determined by DIPA ($n = 3$).

Figure 3 (a, b), respectively. Interestingly, the relatively high contrast of the shell with respect to the core in the image confirms the hollow structure of the pristine urchin-like SFP microspheres (Figure 3 (a)). Compared to the pristine SFP, it is observed that the spike and hollow morphology of the SFP is maintained after attachment of the MWCNTs (Figure 3 (b)). All of the SFP shells have become thicker and have increased in contrast compared with the core. It is therefore concluded that the MWCNTs have successfully coated the surface of the SFP. Based on a collection of >500 analyzed particles in each group, Figure 3 (c) demonstrates that the SFPs after the MWCNT coating have a slight reduction in diameter compared to natural SFPs (ca. 35 μm), which is due to natural SFPs shrinking after freeze drying. By contrast, as presented in Figure 3 (d), the transparency (defined as intensity, where the intensity value ranges from 0–250, with 0 = black and 250 = white) of the SFPs decreased after coating with MWCNTs, which shows that the transparency of the uncoated SFP is greater than that of the coated SFP. Moreover, the aspect ratio and circularity curves of SFP before and after MWCNT coating, as shown in Figure S3, support that the hierarchical biocompatible composite materials maintain good uniformity as the high-density MWCNT coating has been synthesized by a simple method.

The optical images and spectrum of COOH-MWCNT, pristine SFP and MWCNT-SFP composite materials are presented in Figure 4 in order to provide information on component changes during the preparation process. For the acid-treated MWCNTs (Figure 4 (a)), two characteristic peaks centered at

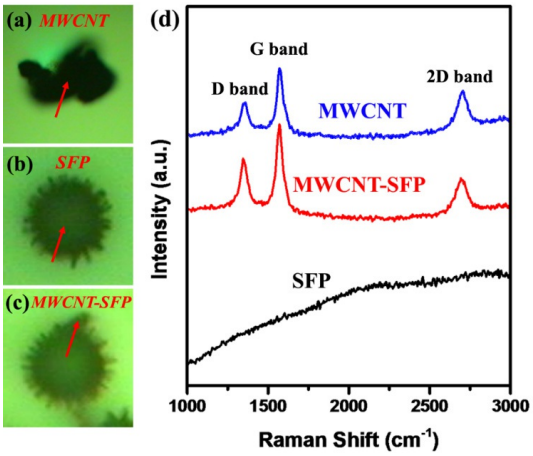

Figure 4. Optical images (a–c) and spectrum (d) of pristine MWCNT, SFP and MWCNT-coated SFP. The red arrows represent the corresponding test position of the three samples, respectively.

1350 and 1585 cm^{-1} are related to the D (disordered carbon) and G (graphitic carbon) bands, as presented in Figure 4 (d).[16] The high G/D intensity ratio (ca. 1.9) indicates the graphitic nature of large-diameter MWCNTs.[17] For pristine SFPs (Figure 4 (b)), no obvious characteristic peaks can be observed. With the MWCNT coating on the SFPs (Figure 4 (c)), the MWCNT-coated SFP composite exhibits a similar G/D ratio (ca. 1.6), confirming that MWCNTs were present on the deposited SFPs. It is noteworthy that after MWCNT-SFP integration, the intensity of the G peak is decreased which may be due to the presence of the SFP assembly. Moreover, the I_D/I_G ratio of the MWCNT-coated SFP composites decreased in comparison to that of the COOH-MWCNTs, which has been previously explained according to defects and structural disorder of carbon nanotubes.[17,18]

Recently, increased efforts mainly focused on imparting biocompatible polymers with electronic sensing properties have sparked widespread application for products such as lithium batteries, supercapacitors, polyactuators, biosensors and flexible transparent electrodes.[19] CNT-coated polymers can be transformed from insulating polymers to conductive composites due to the superior electrical conductivity, excellent biocompatibility and unique physical and chemical properties of MWCNTs and thus can remove restrictions on what other fields these materials can be applied in.[20] Figure 5 shows the current-voltage (I–V) curves of pristine SFP and MWCNT-coated SFP composites. The inset in Figure 5 depicts the corresponding schematic diagram of the measurement device. The detailed fabrication processes of the device are explained in Figures S4 and S5. The resistance value decreased dramatically from 2.05×10^{10} Ω for pristine SFP to 1.01×10^{7} Ω for the MWCNT-coated SFP, implying that the introduction of MWCNTs results in the transformation of the SFP from an insulator to a semiconductor. The corresponding I–V curve of pristine COOH-MWCNTs exhibits high electrical conductivity as shown in Figure S6. Taken together with their abundance, durability, and highly uniform features, MWCNT-functionalized SFP composites show great promise for electrical sensing applications.

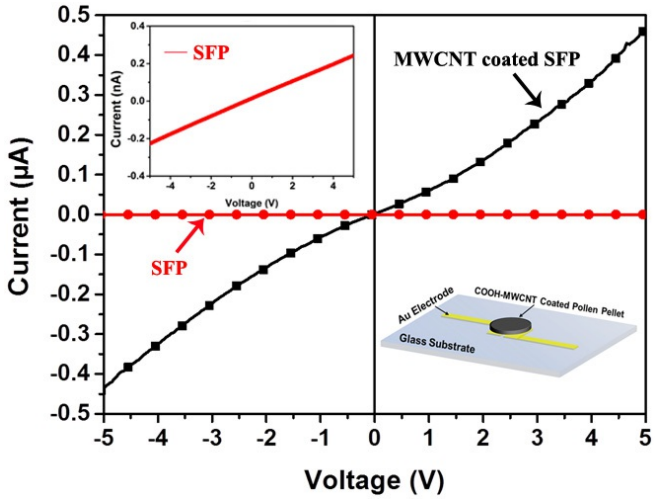

Figure 5. Current–voltage (*I–V*) curves from COOH-MWCNT-coated and uncoated SFPs. The inset images show a COOH-MWCNT-coated pollen pellet between Au electrodes (lower right) and the *I–V* curve of pristine SFP (upper left). Data are representative of three independent measurements.

In summary, we present a facile strategy based on hierarchical self-assembly in order to prepare a highly monodisperse, electroactive biocompatible material based on the combination of natural SFP microcapsules and carbon materials (MWCNTs). The two-step fabrication process combines electrostatic and nonelectrostatic interactions in order to optimize the coating process. Based on this strategy, high-density MWCNT coatings on the surface of SFPs could be achieved by identifying an optimal pH condition to promote surface adsorption. Monodisperse MWCNTs randomly deposited on the SFP surface endowed the microcapsule with excellent electrical properties. Additional research may open up new prospects for fabricating advanced composites based on various robust biomaterials for multipurpose applications.

Experimental Section

Chemicals: COOH-functionalized multiwalled carbon nanotubes (COOH-MWCNTs) with outer diameter of 5–15 nm were purchased from US Research Nanomaterials, Inc. (TX, USA). Natural sunflower pollen grains as defatted were procured from Greer Labs (NC, USA), and pollen defatting indicates washing of pollen grains using ACS grade ethyl ether. Sodium dodecyl sulfate (SDS), cetyltrimethyl ammonium bromide (CTAB) were purchased from Sigma (Singapore). Milli-Q water (Millipore Corp., MA, USA) with a resistivity of 18 MΩ cm was used in all experiments.

Fabrication of COOH-MWCNT-coated sunflower pollen grains: The coating of COOH-MWCNTs onto pollen grains was optimized by initially suspending 100 mg of pollen grains in surfactant (10 mM SDS and 2 mM CTAB). These suspensions were stirred in order to form a uniform dispersion by using magnetic bar and stirrer (RCT, IKA, Germany). In this process, the surfactant concentration was above the critical micelle concentration (CMC) to facilitate surfactant coverage on pollen grains. After one hour stirring, the pollen grains were collected by centrifuge at 4500 rpm and residual surfactant was removed by washing with Milli-Q water. COOH-MWCNTs were dispersed in different pH solutions (pH 3.0, 7.0 and 11.0) by using an ultrasonic generator. The surfactant-coated pollen grains were added into the COOH-MWCNT solutions under bath ultrasonication, further sonication is continued for up to three hours to ensure adsorption of COOH-MWCNTs onto the pollen grains. The COOH-MWCNT-coated pollen grains were collected by centrifugation and dried in a freeze dryer (Labconco, USA) for up to 24 h.

Characterization experiments: The morphologies and structures of the samples were characterized using a FESEM 7600F (JEOL, Japan). Samples were coated with a platinum layer (thickness of 10 nm) by using a JFC-1600 (JEOL, Japan) (20 mA, 60 sec) and images were recorded by employing FESEM with an acceleration voltage of 5.00 kV at different magnifications to provide morphological information before and after MWCNT coating onto pollen grains. The Raman spectra was acquired using a confocal Raman microscope (WITec, Ulm, Germany) with 488 nm laser excitation with a spatial resolution of 1 μm and accumulation time of 3 s at each spot. Spectra for pollen grains, pristine COOH-MWCNT and COOH-MWCNT-coated pollen grains were collected and the data is representative of three independent measurements. The micromeritic properties of all samples were evaluated by dynamic image particle analysis (DIPA).

***Current-voltage (I-V) measurements*:** The pellets were prepared using pollen grains, pristine COOH-MWCNT and COOH-MWCNT-coated pollen grains. The pellets were formed by compressing 150 mg material in a 13 mm stainless steel die with a hydraulic press at 5 ton pressure for 20 s (area 132.75 mm^2; 370 MPa). *I–V* characterization of the pellet samples was conducted using a probe station (Cascade Microtech, OR, USA) with a Keithley 4200-SCS.

Acknowledgements

We acknowledge support from the National Research Foundation Fellowship (NRF-NRFF2011-01) and the National Research Foundation (NRF) Competitive Research Programme (NRF-CRP10-2012-07) grant.

Keywords: carbon nanotubes · biointerfaces · nanoelectronics · pollen capsules

[1] a) C. Kim, X. Y. Liu, *Int. J. Mod. Phys. B* **2006**, *20*, 3727–3732; b) M. T. Byrne, Y. K. Gun'ko, *Adv. Mater.* **2010**, *22*, 1672–1688; c) J. H. Zou, H. Chen, A. Chunder, Y. X. Yu, Q. Huo, L. Zhai, *Adv. Mater.* **2008**, *20*, 3337–3341.

[2] S. Q. Huang, L. Li, Z. B. Yang, L. L. Zhang, H. Saiyin, T. Chen, H. S. Peng, *Adv. Mater.* **2011**, *23*, 4707–4710.

[3] J. H. Yang, T. Xu, A. Lu, Q. Zhang, Q. Fu, *J. Appl. Polym. Sci.* **2008**, *109*, 720–726.

[4] a) D. Tasis, N. Tagmatarchis, A. Bianco, M. Prato, *Chem. Rev.* **2006**, *106*, 1105–1136; b) S. Bredeau, S. Peeterbroeck, D. Bonduel, M. Alexandre, P. Dubois, *Polym. Int.* **2008**, *57*, 547–553; c) P. Liu, *Eur. Polym. J.* **2005**, *41*, 2693–2703.

[5] a) M. R. Weatherspoon, M. B. Dickerson, G. Wang, Y. Cai, S. Shian, S. C. Jones, S. R. Marder, K. H. Sandhage, *Angew. Chem. Int. Ed.* **2007**, *46*, 5724–5727; *Angew. Chem.* **2007**, *119*, 5826–5829; b) S. Y. Chia, J. Urano, F. Tamanoi, B. Dunn, J. I. Zink, *J. Am. Chem. Soc.* **2000**, *122*, 6488–6489; c) J. Y. Huang, X. D. Wang, Z. L. Wang, *Nano Lett.* **2006**, *6*, 2325–2331; d) S. R. Hall, H. Bolger, S. Mann, *Chem. Commun.* **2003**, 2784–2785.

[6] H. P. Li, B. Wang, X. Y. He, J. Xiao, H. S. Zhang, Q. Liu, J. Y. Liu, J. Wang, L. H. Liu, P. Wang, *J. Mater. Chem. A* **2015**, *3*, 9754–9762.

[7] Y. Xia, W. K. Zhang, Z. Xiao, H. Huang, H. J. Zeng, X. R. Chen, F. Chen, Y. P. Gan, X. Y. Tao, *J. Mater. Chem.* **2012**, *22*, 9209–9215.

[8] L. L. Wang, T. Fei, Z. Lou, T. Zhang, *ACS Appl. Mater. Interfaces* **2011**, *3*, 4689 – 4694.
[9] S. J. Yang, D. L. Meng, J. H. Sun, Y. Huang, Y. Huang, J. X. Geng, *ACS Appl. Mater. Interfaces* **2014**, *6*, 7686 – 7694.
[10] a) R. H. Baughman, A. A. Zakhidov, W. A. de Heer, *Science* **2002**, *297*, 787 – 792; b) J. N. Coleman, U. Khan, W. J. Blau, Y. K. Gun'ko, *Carbon* **2006**, *44*, 1624 – 1652.
[11] S. J. Yang, D. L. Meng, J. H. Sun, W. P. Hou, Y. B. Ding, S. D. Jiang, Y. Huang, Y. Huang, J. X. Geng, *RSC Adv.* **2014**, *4*, 25051 – 25056.
[12] L. Y. Zhu, Y. C. Han, M. Z. Tian, Y. L. Wang, *Langmuir* **2013**, *29*, 12084 – 12092.
[13] M. A. Karimi, R. Behjatmanesh-Ardakani, A. A. Goudi, S. Zali, *J. Braz. Chem. Soc.* **2008**, *19*, 1523 – 1530.
[14] a) P. Gilli, L. Pretto, V. Bertolasi, G. Gilli, *Acc. Chem. Res.* **2009**, *42*, 33 – 44; b) A. Di Crescenzo, R. Germani, E. Del Canto, S. Giordani, G. Savelli, A. Fontana, *Eur. J. Org. Chem.* **2011**, 5641 – 5648.
[15] F. Fornasiero, H. G. Park, J. K. Holt, M. Stadermann, C. P. Grigoropoulos, A. Noy, O. Bakajin, *Proc. Natl. Acad. Sci. USA* **2008**, *105*, 17250 – 17255.
[16] T. Muraliganth, A. V. Murugan, A. Manthiram, *Chem. Commun.* **2009**, 7360 – 7362.
[17] K. Fu, O. Yildiz, H. Bhanushali, Y. X. Wang, K. Stano, L. G. Xue, X. W. Zhang, P. D. Bradford, *Adv. Mater.* **2013**, *25*, 5109 – 5114.
[18] Y. C. Dong, K. C. Yung, R. G. Ma, X. Yang, Y. S. Chui, J. M. Lee, J. A. Zapien, *Carbon* **2015**, *86*, 310 – 317.
[19] a) A. Mierczynska, M. Mayne-L'Hermite, G. Boiteux, J. K. Jeszka, *J. Appl. Polym. Sci.* **2007**, *105*, 158 – 168; b) K. T. Lau, H. Y. Cheung, J. Lu, Y. S. Yin, D. Hui, H. L. Li, *J. Comput. Theor. Nanosci.* **2008**, *5*, 23 – 35; c) I. Y. Jeon, H. J. Lee, Y. S. Choi, L. S. Tan, J. B. Baek, *Macromolecules* **2008**, *41*, 7423 – 7432; d) H. D. Bao, Z. X. Guo, J. Yu, *Polymer* **2008**, *49*, 3826 – 3831; e) C. J. Zhou, S. F. Wang, Q. X. Zhuang, Z. W. Han, *Carbon* **2008**, *46*, 1232 – 1240.
[20] B. L. Wardle, D. S. Saito, E. J. Garcia, A. J. Hart, R. G. de Villoria, E. A. Verploegen, *Adv. Mater.* **2008**, *20*, 2707 – 2714.

Manuscript received: January 8, 2016
Accepted Article published: February 22, 2016
Final Article published: March 3, 2016